

Nanoscale

Accepted Manuscript



This is an *Accepted Manuscript*, which has been through the Royal Society of Chemistry peer review process and has been accepted for publication.

Accepted Manuscripts are published online shortly after acceptance, before technical editing, formatting and proof reading. Using this free service, authors can make their results available to the community, in citable form, before we publish the edited article. We will replace this *Accepted Manuscript* with the edited and formatted *Advance Article* as soon as it is available.

You can find more information about *Accepted Manuscripts* in the [Information for Authors](#).

Please note that technical editing may introduce minor changes to the text and/or graphics, which may alter content. The journal's standard [Terms & Conditions](#) and the [Ethical guidelines](#) still apply. In no event shall the Royal Society of Chemistry be held responsible for any errors or omissions in this *Accepted Manuscript* or any consequences arising from the use of any information it contains.

ARTICLE

Layered Zinc Hydroxide Nanocones: Synthesis, Facile Morphological and Structural Modification, and Properties

Cite this: DOI: 10.1039/x0xx00000x

Wei Ma,^{abc} Renzhi Ma,^{*a} Jianbo Liang,^a Chengxiang Wang,^a Xiaohe Liu,^{*b} Kechao Zhou,^{*c} Takayoshi Sasaki^aReceived 00th January 2012,
Accepted 00th January 2012

DOI: 10.1039/x0xx00000x

www.rsc.org/

Layered zinc hydroxide nanocones intercalated with DS⁻ have been synthesized for the first time *via* a convenient synthetic approach of homogeneous precipitation in the presence of urea and sodium dodecyl sulfate (SDS). SDS plays a significant role in controlling the morphologies of as-synthesized samples. Conical samples intercalating various anions were transformed through anion-exchange route in ethanol solution and the original conical structure was perfectly maintained. Instead, these DS⁻-inserted nanocones can be transformed into square-like nanoplates in aqueous solution at room temperature and cater the demand of different morphology-dependent properties. Corresponding ZnO nanocones and nanoplates have been further obtained through thermal calcination of NO₃⁻-intercalating zinc hydroxide nanocones/nanoplates. These ZnO nanostructures with different morphologies exhibit promising photocatalytic properties.

Introduction

Layered metal hydroxide salts, in a general formula of M^{II}(OH)_{2-x}Aⁿ⁻_{x/n}·mH₂O (or M^{II}_{1-x/2}(OH)₂Aⁿ⁻_{x/n}·mH₂O) in which OH⁻ deficiency on the host layers is compensated by coordinated/grafted guest anions (Aⁿ⁻), is one of relatively rare anion-exchangeable hosts in addition to well-known layered double hydroxides (LDH, M^{II}_{1-x}M^{III}_x(OH)₂Aⁿ⁻_{x/n}·mH₂O). They have attracted extensive interests because of a rich interlayer chemistry interacting with both inorganic/organic anions and potential applications in many fields such as drug delivery agents, catalyses, supercapacitors.¹⁻⁷ In this category, layered zinc hydroxide salts (Typical formula: Zn₅(OH)₈Aⁿ⁻_{2/n}·mH₂O, A = Cl⁻, NO₃⁻, etc.) is regarded as one of the most representative structures. The host layers are composed of both octahedral and tetrahedral coordination. Specifically, approximate one quarter of octahedral metal positions are vacant, and a pair of tetrahedral metal atoms, located above and below the missing octahedra, directly coordinate with anions in the interlayer gallery.⁸⁻¹⁰ The anion exchangeability endows their uses as drug carriers with controllable release rate due to a low cytotoxicity in acidic environment.¹¹⁻¹⁶ In addition, layered zinc hydroxide is also widely used as a precursor for preparation of ZnO, an important semiconductor with a large band gap (3 ~ 4.5 eV) and a high exciton binding energy (60 ~ 100 meV). ZnO transformed from layered zinc hydroxide *via* environment-friendly thermal decomposition route has been thoroughly exploited owing to the peculiar physical and chemical properties dependent on the size, morphology and orientation.¹⁷⁻²⁰ Moreover, ZnO was also revealed as a promising photocatalyst with high photosensitivity and nontoxic nature, which might contribute to solve environmental

problems for its strong oxidizing power and solar energy conversion capability.²¹⁻²³ Layered zinc hydroxides, through a cost-efficient procedure, can also be used to synthesize mesoporous ZnO nanomaterials with superhigh specific surface in an industrial scale. Nevertheless, layered zinc hydroxide salts are known for their instability in aqueous solution even at room temperature. In fact, there are very few studies dedicated to the morphological control of layered zinc hydroxide salts with various interlayer anions or resulting ZnO obtained through calcination.^{17,24-26}

On the other hand, cylindrical nanotubes and conical nanocones formed by rolling-up of layered lamellae or nanosheets, exhibiting high aspect ratio and hollow interior, have been the star materials over the past decade due to fascinating morphology-dependent properties and applications such as nanoelectronic and optoelectronic devices, solar cells, and environmental protection, etc.²⁷⁻³¹ Nevertheless, except carbon and boron nitride, and cobalt or nickel hydroxide systems reported very recently, there are seldom successes in synthesizing large quantities of nanocones from other layered structures.³²⁻³⁵

In current work, we demonstrate a synthetic strategy capable of producing unique zinc hydroxide nanocones in large quantities. Similar to our previous reports on cobalt or nickel hydroxide systems,³³⁻³⁵ layered zinc hydroxide nanocones could be synthesized utilizing urea as a slowly-releasing alkaline source together with anionic surfactants such as sodium dodecyl sulfate (C₁₂H₂₅OSO₃Na, SDS) *via* an oil-bath synthetic procedure. It was found that SDS not only directly determined the interlayer spacing through intercalation, but also affected the morphology of as-prepared layered zinc hydroxide products. DS⁻-intercalated nanocones undergo exchange reaction with

different anions (Cl^- , NO_3^- , CH_3COO^-) in ethanol. However, the nanocone morphology would not maintain if the same exchange reaction was carried out in aqueous solution at room temperature, instead transforming into square-like nanoplates. This aspect reveals a unique feature of zinc hydroxide for facile morphology manipulation and thus provides a novel transformation protocol under a mild condition, e.g., at room temperature. Furthermore, ZnO nanocones and nanoplates could be attained *via* calcination of corresponding layered zinc hydroxide precursors intercalating nitrate anions. Under the irradiation of UV light, ZnO nanocones and nanoplates were revealed to exhibit remarkable photocatalytic properties in decomposing organic dyes.

Materials and methods

Materials

All reagents used were of analytical grade and were purchased from Wako Chemical Reagents Company, Japan. Milli-Q water was utilized throughout the experiments.

Synthesis

Synthesis of layered zinc hydroxide nanocones. In a typical synthetic procedure, $\text{Zn}(\text{NO}_3)_2 \cdot 6\text{H}_2\text{O}$, urea and SDS were dissolved in a 1000 cm^3 two-neck flask with Milli-Q water under nitrogen gas, yielding the concentrations of 5 mM, 10 mM and 25 mM, respectively. Then, the mixed solution was heated at the refluxing temperature for 5.5 h under continuous magnetic stirring. The final product was recovered by washing with Milli-Q water and ethanol several times and air-dried at room temperature.

Anion-exchange reaction. As-synthesized layered zinc hydroxide nanocones with DS^- was dispersed into 100 cm^3 of ethanol containing 25 mmol NaNO_3 , NaCl and CH_3COONa , respectively. The vessels were tightly capped and mechanically shaken for several hours at room temperature. The products were filtered and air-dried at room temperature.

Transformation of zinc hydroxide nanocones to nanoplates. The layered zinc hydroxide nanocones were dispersed into 200 cm^3 of 1 M NaCl aqueous solution without any agitation for 24 h at room temperature. The samples were collected by filtering, washing, and air-dried at room temperature.

Synthesis of ZnO nanocones and nanoplates. The as-prepared layered zinc hydroxide nanocones and nanoplates in NO_3^- form were calcined at a heating rate of 1°C in air to 200°C and 800°C .

Evaluation of photocatalytic performance. 100 mg of ZnO nanocones or nanoplates were dispersed in 50 ml aqueous methylene blue (MB) with concentration of 15 mg/L. The adsorption of MB on the surface of the photocatalysts was facilitated under the magnetic stirring in the dark for 1 h. A 500 W Xe lamp (XEF-501S San-ei Electric) was used for UV irradiation of samples. Samples were placed at $\sim 10 \text{ cm}$ from the light source, corresponding to a UV intensity of approximately 1 mW/cm^2 at $\lambda < 300 \text{ nm}$, as determined with a spectroradiometer (USR-30 Ushio Electric). The UV-Vis absorption spectrum of the aqueous solution of MB was recorded using a Hitachi U-4100 UV-vis spectrophotometer.

Characterization

The phase identification of the as-prepared samples were conducted by X-ray diffraction (XRD, Rigaku Ultima IV diffractometer) operated at 40 kV/40 mA with $\text{Cu-K}\alpha$ radiation.

The morphology and dimension of as-prepared products were characterized on a JSM-6010LA scanning electron microscope (SEM). High-resolution transmission electron microscopy (HRTEM) images and selected area electron diffraction (SAED) patterns were obtained on a JEM-3000F TEM.

Metal contents were determined by inductively coupled plasma (ICP) atomic emission spectroscopy (SPS1700HVR, Seiko Instruments) after dissolving a weighed amount of sample with an aqueous HCl solution.

Thermogravimetric analysis (TGA) measurements were carried out using a Thermo Plus 2 TG8120 instrument in a temperature range of room temperature- 1000°C at a heating rate of 1°C min^{-1} under air flow.

Results and discussion

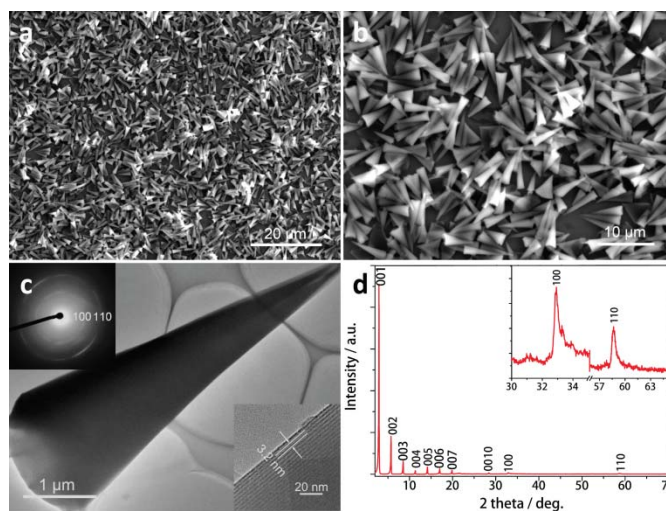


Figure 1. a) Low- and b) High-magnification SEM images of as-prepared layered hydroxide nanocones. c) TEM image of resulting nanocones. The inset in (c) shows an SAED pattern and HRTEM image taken on an individual nanocone. d) XRD pattern of as-synthesized zinc hydroxide nanocones intercalated with DS^- anion (Inset) magnified profile in the region of $30\text{--}35^\circ$ and $55\text{--}65^\circ$.

Figure 1a&b exhibit typical scanning electron microscopy (SEM) images at different magnifications of as-prepared zinc hydroxide nanocones obtained through oil-bath precipitation of zinc nitrate (5 mM) in the presence of urea (10 mM) and SDS (25 mM). It can be seen that a large quantity of uniform conical objects were synthesized. The length of as-obtained zinc hydroxide nanocones is around several micrometers, whereas the average tip and bottom diameters are approximately $0.2 \mu\text{m}$ and $2 \mu\text{m}$, respectively. The hollow interior structure is confirmed by transmission electron microscopy (TEM) image as shown in Figure 1c. A contrast difference is discernible between the dark periphery and greyish intermediate portion. The wall thickness of these nanocones is about several hundreds of nanometres. The selected area electron diffraction (SAED) pattern on individual nanocone is given in the top-left inset of Figure 1c, which can be readily indexed to in-plane or $[001]$ zone-axis diffraction of hexagonal zinc hydroxide with a lattice constant of $a = 0.32 \text{ nm}$. The diffraction rings with d -spacings of 0.27 nm and 0.16 nm correspond to $[100]$ and $[110]$, indicating the rolling-up of hydroxide layers lack of

crystallographic interlayer registry. The layered stacking with an interlayer spacing of approximately 3.2 nm is visualized by the high-resolution transmission electron microscopy (HRTEM) given in the bottom-right inset of Figure 1c.

Typical X-ray Diffraction (XRD) pattern of as-prepared nanocones intercalating DS⁻ anions is displayed in Figure 1d. All the diffraction peaks can be indexed in a hexagonal cell of $a = 0.3150$ (2) nm, $c = 3.1532$ (8) nm, consistent with layered zinc hydroxides reported in literature.³⁶⁻³⁸ Sharp (00 l) basal reflections at low angular range of XRD pattern reveal a high crystallinity feature of the sample along the layer stacking direction (c axis). The in-plane diffraction peaks around 33° and 59° in the magnified XRD pattern in the top-right inset of Figure 1d indicate that layered zinc hydroxide was synthesized by this convenient route. The basal spacing close to 3.2 nm indicates that the DS⁻ anions are likely to arrange in bilayers similar to previous reports.^{1,39} The basal spacing (d_L) for DS⁻ bilayers in the hydroxide gallery may be expressed as: $d_L = (0.73 + 2 \times 0.15 + 2 \times 0.197) + 2 \times 0.127 \times 12 \sin \theta$, where the thickness of host layer is taken as 0.73 nm, the carbon chain length of dodecyl sulphate is around $0.127n$ nm ($n = 12$), a sulphate head of 0.197 nm and an end tail of 0.15 nm, respectively.^{1,40} As a result, the tilting angle of the bistratal DS⁻ chains can be estimated as approximate 35°. According to the result of wet chemical analyses as well as thermogravimetric analysis (TGA) shown in Figure S1, the chemical composition of as-prepared nanocones was estimated as $Zn(OH)_{1.55}DS_{0.45} \cdot 0.3H_2O$ (Anal. calcd: Zn, 30.2%; S, 6.7%; ignition loss, 62.4%. Found: Zn, 28.9%; S, 6.31%; ignition loss, 61.8%). The data indicate that the nanocones are layered zinc hydroxide salts with a composition very close to the theoretical formula of $Zn_5(OH)_8DS_2 \cdot 2H_2O$.

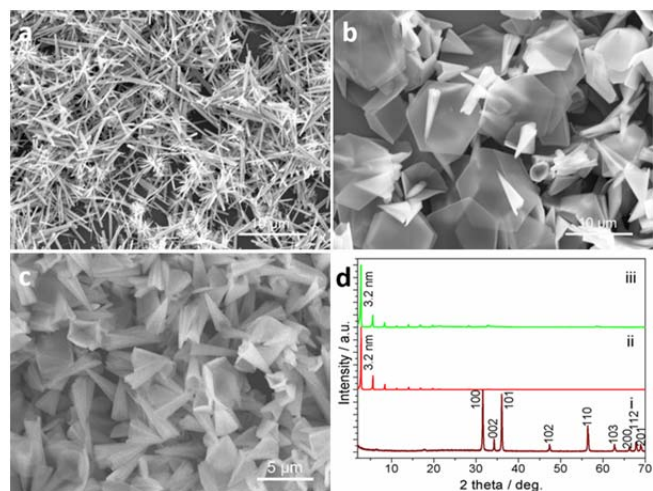


Figure 2. SEM images of as-prepared samples obtained with different quantity of SDS, a) 0. b) 12.5 mM. c) 50 mM. And d) corresponding XRD pattern (i) 0, (ii) 12.5 mM, (iii) 50 mM.

The amount or concentration of SDS surfactant has a great influence on the morphology and phase of as-prepared products. Without using a surfactant, the products evolved into ZnO nanorods. Figure 2a depicts a typical SEM image of uniform nanorods with a length of approximate 5 μ m. XRD pattern shown in Figure 2d(i) revealed a hexagonal ZnO structure with lattice constants of $a = 0.3259$ (1) nm and $c = 0.5224$ (4) nm. When 12.5 mmol of SDS was used, the majority of the product appeared as hexagonal nanoplates, albeit a small fraction of nanocones was also observed (Figure 2b). With increasing the amount of SDS to 25 mM, high-purity nanocones were

synthesized (Figure 1a). Further increasing the amount to 50 mM, nanocones were still obtained as the main product as presented in Figure 2c. Figure 2d compares the XRD patterns of as-obtained samples under different SDS concentration, which indicates the formation of layered zinc hydroxide salts with similar interlayer spacing under varied amount of SDS. We speculate that SDS works as both surfactant and structure-directing agent for the formation of peculiar nanocones of layered zinc hydroxides, the same with earlier reports on Co-(Ni) hydroxides.³⁴ Relatively low energy barrier with a tubular structure is responsible for the rolling-up of a thin sheet/layer along a conical angle into a nanocone under the template role of SDS.⁴¹

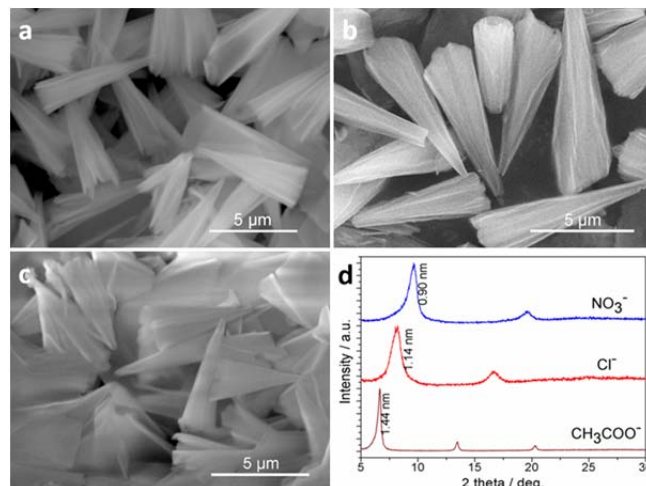


Figure 3. SEM images of zinc hydroxide nanocones exchanged with different anions in ethanol. a) NO₃⁻. b) Cl⁻. c) CH₃COO⁻. d) XRD pattern of zinc hydroxide nanocones exchanged with different anions.

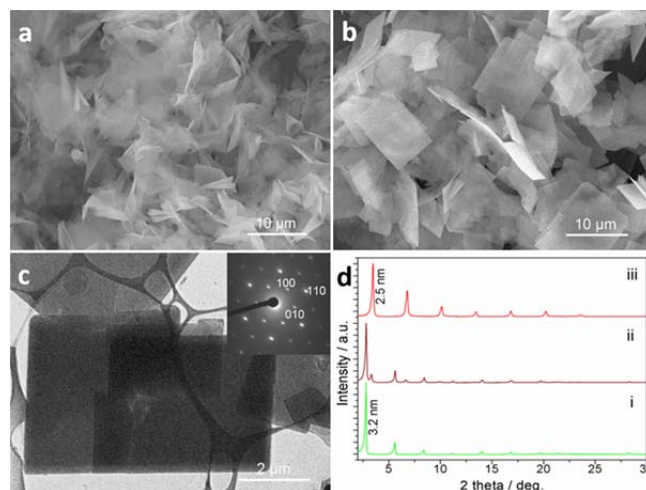


Figure 4. SEM images of zinc hydroxide in contact with aqueous NaCl (1 M) solution for different durations, a) 6 h. b) 24 h. c) TEM image of as-transformed square plates at 24 h (Inset) SAED pattern. d) XRD pattern of transformed products in NaCl solution for different durations (i) 0 h, (ii) 6 h, (iii) 24 h.

Figure 3a-c exhibit SEM images of layered zinc hydroxide nanocones exchanged with NO₃⁻, Cl⁻ and CH₃COO⁻ using ethanol as the solvent at room temperature. Figure 3d displays the XRD patterns of zinc hydroxide nanocones intercalated with Cl⁻, NO₃⁻ and

CH₃COO⁻ anions. The interlayer spacing shifted to 0.90 nm for NO₃⁻, 1.14 nm for Cl⁻ and 1.44 nm for CH₃COO⁻, respectively, from original 3.15 nm for DS⁻ anions. Compared with the previous report on layered Co-(Ni) hydroxide nanocones intercalating NO₃⁻ (0.79 nm), Cl⁻ (0.78 nm) and CH₃COO⁻ (0.91 nm), the interlayer spacing of current zinc hydroxide nanocones is noticeably larger. The reason is not clear yet. We speculate that the exchange in different solvents, e.g., in ethanol or in water, might contribute to different anion arrangement and consequently interlayer spacings. In fact, the interlayer spacing was reduced to 0.79 nm for the exchange with Cl⁻ if the anion-exchange process was carried out by using 1M NaCl in ethanol/water binary solvents (1:1 v/v) (Figure S2). However, the nanocone morphology could not be well retained when water was added in the solvents. It was found that the nanocones were deteriorated into irregular nanoplates in the deionized water (Figure S3a). In Figure 4a&b, the conical structure was gradually transformed into monodisperse square-like nanoplates in aqueous 1 M NaCl solution. The lateral length of the square-like plates is approximate 4 ~ 5 μm, while a very thin and uniform thickness is estimated to be a few tens of nm. The same morphological change was also observed in aqueous 1 M NaNO₃ solution (Figure S3b). SAED pattern collected on individual nanoplate shown in the inset of Figure 4c confirmed the single-crystal nature with hexagonally arranged diffraction spots. The slight deviation from an ideal hexagonal symmetry, e.g., into an orthorhombic one, which might be attributed to an occupancy fluctuation or position shift of the Zn²⁺ in the hydroxide layer, is considered to be responsible for the formation of rectangular platelets. XRD patterns in Figure 4d show that the interlayer spacing was reduced to 2.5 nm from original 3.2 nm, revealing a partial de-intercalation of DS⁻ and possible transformation of a bilayer to monolayer arrangement in the gallery. The less DS content was supported by smaller weight loss in TG analysis (Figure S4a). In other words, the anion-exchange process was not fully facilitated in aqueous solutions for zinc hydroxide nanocones, which is significantly different from the previous reports on Co-(Ni) hydroxide nanocones.³³⁻³⁵ Such a unique feature of Zn-based hydroxide nanostructures may be effectively used to apply facile morphological and structural modification at room temperature.

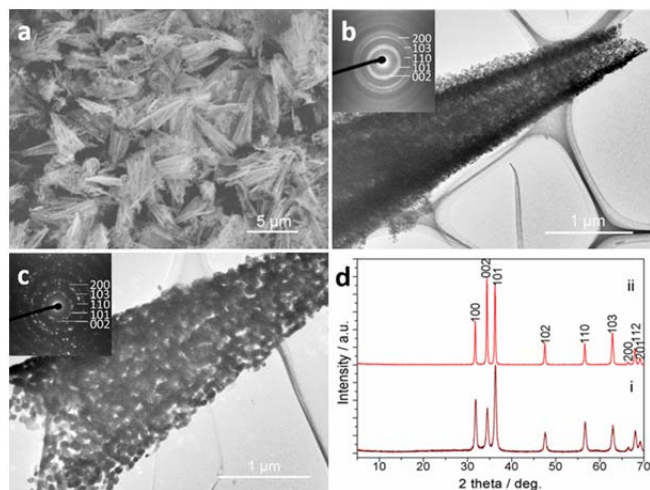


Figure 5. a) SEM and b) TEM images of ZnO nanocones obtained at 200 °C (Inset) SAED pattern. c) TEM image of ZnO nanocones obtained at 800 °C (Inset) SAED pattern. d) XRD pattern of ZnO nanocones obtained at different temperature (i) 200 °C, (ii) 800 °C.

The layered zinc hydroxide nanocones could be transformed into ZnO nanocones *via* simple calcination treatment. In

particular, inorganic anions (e.g., NO₃⁻) intercalated hydroxide nanocones show lower pyrolysis temperature and release less gas content during the calcination, as confirmed by TG analysis in Figure S4b. They are more suitable for thermal transformation into ZnO nanocones. To well preserve original nanocones structure, a slow heating rate was also found favourable. Figure 5 shows the SEM, TEM images and XRD pattern of ZnO nanocones obtained by calcination at different temperature. The average diameter of ZnO nanocones is smaller than starting hydroxide nanocones owing to dehydration and removal of anionic species in the galleries through pyrolysis. The hollow interior nature of nanocones was identified by TEM characterizations in Figure 5b and c. In general, the oxide nanocones are polycrystalline, being composed of many tiny particles. The interstices between them may be formed due to the release of foamed water and gas contents. With the increase of calcination temperature to 800 °C, the polycrystalline nanoparticle assembly into a conical framework is obvious (Figure 5c). XRD patterns of calcined nanocones obtained at different temperature given in Figure 5d can be both indexed to be hexagonal ZnO with almost the same lattice constants ($a = 0.32466$ (4) nm and $c = 0.5197$ (4) nm for 200 °C, $a = 0.32517$ (7) and $c = 0.5205$ (2) nm for 800 °C).

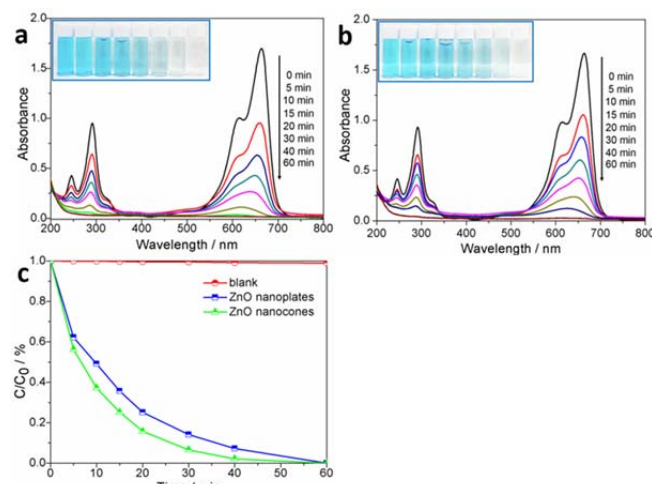


Figure 6. Evolution of absorption spectra of methylene blue (15 mg/L, 50 ml) with different photocatalysts. a) ZnO nanocones. b) ZnO nanoplates. Insets in both panels show photographs of the methylene blue suspensions corresponding to different UV illumination time. c) time-dependent photodegradation of methylene blue.

The photocatalytic performance of ZnO nanocones and nanoplates were evaluated through examining the photodegradation of methylene blue (MB) as a representative pollutant under irradiation of ultraviolet (UV) light. The time-dependence of UV-Vis absorption spectra of the aqueous solution of MB with 100 mg of ZnO nanocones and nanoplates is compared in Figure 6. As can be seen from Figure 6a and b, well-defined absorption peaks of MB positioned at 610 nm and 660 nm rapidly decreased with prolonged time duration. MB was almost completely degraded in an hour verified by both UV-Vis absorption spectra and photographs shown in the insets of Figure 6a and b. Compared with blank experiment without a photocatalyst, the remarkable efficiency of photodegradation within one hour by using ZnO nanocones and nanoplates is evident (Figure 6c). Furthermore, the photocatalytic efficiency of ZnO nanocones appears higher than that of ZnO nanoplates. As the band structure of these ZnO nanomaterials should not

differ too much, the reason might be derived from their morphological difference, e.g., specific surface area, exposed crystal facets, etc. It seems that ZnO nanocones exhibit higher specific surface area than that of nanoplates due to a porous assembly of nanoparticles. Furthermore, it is known that the efficiency of photocatalysis is significantly affected by the specific exposed crystal facets. It has been reported that (002) polar face of ZnO possesses higher activity than that of (100). Consequently, the catalytic activity of hexagonal ZnO would be enhanced with more exposed (002) facets. Based on XRD patterns for ZnO nanocones in Figure 5d(ii) and ZnO nanoplates in Figure S5, the peak intensity ratios were tabulated in Table S1. It can be seen that the peak intensity ratio of (100) to (002) is higher in ZnO nanocones than that in ZnO nanoplates. In other words, nanoplates hold preferred growth tendency oriented along *c* axis, which may diminish the proportion of (002) polar faces, namely the exposed (002) facets.⁴²⁻⁴⁵ The above factors might contribute to the reasons for ZnO nanocones to show higher photocatalytic activity than that of ZnO nanoplates. This indicates the high potential of rendering morphological characteristics for functional optimization, as well as employing ZnO with unique nanocones structure for photochemical and optoelectronic applications.

Conclusions

In summary, layered zinc hydroxide nanocones intercalated with DS⁻ anions have been synthesized *via* a convenient and reliable synthetic approach of homogeneous precipitation in the presence of urea and SDS, in which SDS impart a significant influence on synthesis as both surfactant and structure-directing agent. These nanocones could be transformed into square-like nanoplates in aqueous solution even at room temperature. Corresponding ZnO nanocones and nanoplates were synthesized through further calcination, which provide convenient and effective routes to design peculiar conical and plate-like functional oxides under mild conditions. The fine control on morphological feature, e.g., nanocone *vs.* nanoplate, may be employed to tune their properties, e.g., photocatalytic performance. The conical structure with hollow interior as well as its nanoplate counterpart is promising for various applications such as photocatalysis, optoelectronics and biomedicine, etc.

Acknowledgement

The work was supported in part by the World Premier International Center Initiative (WPI) on Materials Nanoarchitectonics, MEXT, Japan. R.M. acknowledges support from JSPS KAKENHI Grant number 24310095. X.L. acknowledges support from National Natural Science Foundation of China (51372279), Hunan Provincial Natural Science Foundation of China (13JJ1005), and Shenghua Scholar Program of Central South University.

Note and references

^a International Center for Materials Nanoarchitectonics (MANA), National Institute for Materials Science (NIMS), Namiki 1-1, Tsukuba, Ibaraki, 305-0044, Japan; E-mail: MA.Renzi@nims.go.jp

^b School of Resources Processing and Bioengineering, Central South University, Changsha 410083, PR China; E-mail: liuxh@csu.edu.cn

^c State Key Laboratory of Powder Metallurgy, Central South University, Changsha 410083, PR China. E-mail: zhoukechao@csu.edu.cn

[†] Electronic Supplementary Information (ESI) available: The typical SEM images, TGA curves and XRD patterns of as-prepared samples. See DOI: 10.1039/b000000x/

- M. Meyn, K. Beneke and G. Lagaly, *Inorg. Chem.*, 1993, **32**, 1209.
- G. R. Williams, J. Crowder, J. C. Burley and A. M. Fogg, *J. Mater. Chem.*, 2012, **22**, 13600.
- V. Laget, C. Hornick, P. Rabu, M. Drillon and R. Ziessel, *Coord. Chem. Rev.*, 1998, **178**, 1533.
- R. Rojas, C. Barriga, M. A. Ulibarri and P. Malet, Rives, V. *J. Mater. Chem.*, 2002, **12**, 1071.
- L. Xu, Y. S. Ding, C. H. Chen, L. Zhao, C. Rimkus, R. Joesten and S. L. Suib, *Chem. Mater.*, 2007, **20**, 308.
- W. K. Hu and D. Noréus, *Chem. Mater.*, 2003, **15**, 974.
- V. Gupta, T. Kusahara, H. Toyama, S. Gupta and N. Miura, *Electrochem. Commun.*, 2007, **9**, 2315.
- W. Stahlin and H. R. Oswald, *Acta Crystallogr., Sect. B*, 1970, **26**, 860.
- R. Ma, Z. P. Liu, K. Takada, K. Fukuda, Y. Ebina, Y. Bando and T. Sasaki, *Inorg. Chem.*, 2006, **45**, 3964.
- A. Moezzi, A. McDonagh, A. Dowd and M. Cortie, *Inorg. Chem.*, 2012, **52**, 95.
- S. Inoue and S. Fujihara, *Inorg. Chem.*, 2011, **50**, 3605.
- L. Poul, N. Jouini and F. Fiévet, *Chem. Mater.*, 2000, **12**, 3123.
- H. Morioka, H. Tagaya, M. Karasu, J. Kadokawa and K. Chiba, *Inorg. Chem.*, 1999, **38**, 4211.
- J. H. Yang, Y. S. Han, M. Park, T. Park, S. J. Hwang and J. H. Choy, *Chem. Mater.*, 2007, **19**, 2679.
- M. Z. Hussein, S. H. Al-Ali, Z. Zainal and M. N. Hakim, *Int. J. Nanomed.*, 2011, **6**, 1373.
- S. H. H. Al-Ali, M. A. Qubaisi, M. Z. Hussein, Z. Zainal and M. N. Hakim, *Int. J. Nanomed.*, 2011, **6**, 3099.
- A. Tsukazaki, A. Ohtomo, T. Onuma, M. Ohtani, T. Makino, M. Sumiya, K. Ohtani, S. F. Chichibu, S. Fuke, Y. Segawa, H. Ohno, H. Koinuma and M. Kawasaki, *Nat. Mater.*, 2005, **4**, 42.
- K. Hümmer, *phys. status solidi (b)*, 1973, **56**, 249.
- X. D. Wang, C. J. Summers and Z. L. Wang, *Nano Lett.*, 2004, **4**, 423.
- A. B. Djuricic and Y. H. Leung, *Small*, 2006, **2**, 944.
- L. Q. Jing, Y. C. Qu, B. Q. Wang, S. D. Li, B. J. Jiang, L. B. Yang, W. Fu, H. G. Fu and J. Z. Sun, *Sol. Energy Mater. Sol. Cells*, 2006, **90**, 1773.
- P. Li, Z. Wei, T. Wu, Q. Peng and Y. Li, *J. Am. Chem. Soc.*, 2011, **133**, 5660.
- C. L. Carnes and K. J. Klabunde, *J. Mol. Catal. A: Chem.*, 2003, **194**, 227.
- M. H. Huang, Y. Y. Wu, H. Feick, N. Tran, E. Weber and P. D. Yang, *Adv. Mater.*, 2001, **13**, 113.
- M. Law, L. E. Greene, J. C. Johnson, R. Saykally and P. D. Yang, *Nat. Mater.*, 2005, **4**, 455.
- E. Kandare and J. M. Hossenlopp, *Inorg. Chem.*, 2006, **45**, 3766.
- K. Tibbetts, R. Doe and G. Ceder, *Phys. Rev. B*, 2009, **80**, 014102.
- S. Berber, Y. K. Kwon and D. Tománek, *Phys. Rev. B*, 2000, **62**, R2291.

- 29 A. Krishnan, E. Dujardin, M. M. J. Treacy, J. Higdahl, S. Lynum and T. W. Ebbesen, *Nature*, 1997, **388**, 451.
- 30 D. Golberg, Y. Bando, Y. Huang, T. Terao, M. Mitome, C. C. Tang and C. Y. Zhi, *ACS Nano*, 2010, **4**, 2979.
- 31 K. Li, J. Ju, Z. Xue, J. Ma, L. Feng, S. Gao and L. Jiang, *Nat. Commun.*, 2013, **4**, 2276.
- 32 L. Bourgeois, Y. Bando, W. Q. Han and T. Sato, *Phys. Rev. B*, 2000, **61**, 7686.
- 33 R. Ma, Y. Bando and T. Sasaki, *J. Phys. Chem. B*, 2004, **108**, 2115.
- 34 X. H. Liu, R. Z. Ma, Y. Bando and T. Sasaki, *Angew. Chem. Int. Ed.*, 2010, **49**, 8253.
- 35 X. H. Liu, R. Ma, Y. Bando and T. Sasaki, *Adv. Mater.*, 2012, **24**, 2148.
- 36 M. Vucelic, G. D. Moggridge and W. Jones, *J. Phys. Chem.*, 1995, **99**, 8328.
- 37 F. Millange, R. I. Walton and D. O'Hare, *J. Mater. Chem.*, 2000, **10**, 1713.
- 38 Y. Zhao, F. Li, R. Zhang, D. G. Evans and X. Duan, *Chem. Mater.*, 2002, **14**, 4286.
- 39 V. V. Naik, R. Chalasani and S. Vasudevan, *Langmuir*, 2011, **27**, 2308.
- 40 C. H. Liang, Y. Shimizu, M. Masuda, T. Sasaki and N. Koshizaki, *Chem. Mater.*, 2004, **16**, 963.
- 41 P. C. Tsai and T. H. Fang, *Nanotechnology*, 2007, **18**, 105702.
- 42 H. Lin, L. Li, M. Zhao, X. Huang, X. Chen, G. Li and R. Yu, *J. Am. Chem. Soc.*, 2012, **134**, 8328.